Some Recent Developments in SPM of Crystalline Polymers

Jamie K. Hobbs*, Alex K. Winkel, Terence J. McMaster, Andrew D.L. Humphris, Andrew A. Baker, Stephen Blakely, Meriem Aissaoui, and Mervyn J. Miles

H. H. Wills Physics Laboratory, Tyndall Avenue, Bristol, BS8 1TL, UK
Tel. 44 (0)117 9288697 Fax. 44 (0)117 9255624
e-mail: jamie.hobbs@bristol.ac.uk

SUMMARY: Some recent advances in the application of atomic force microscopy to crystalline polymers are detailed. Ultra-high resolution imaging of crystal surfaces, combined with the analysis of computer generated Connolly surfaces, enables the unambiguous identification of features on the cellulose crystal surface at near-atomic resolution. The electronic enhancement of the quality factor of the cantilever when tapping in liquids enables a considerable improvement in force sensitivity to be obtained, allowing the fully saturated surface of an isotactic polystyrene gel to be imaged under the solvating molecule, at nanometre resolution. A series of experiments are detailed in which processes such as crystallization, crystal thickening and crystal deformation are followed *in situ*, in real time, providing significant new insights into long standing problems in polymer science.

Introduction

Scanning probe microscopy (SPM) is a family of a dozen or more microscopies based on the concept and technology of the founding member, scanning tunnelling microscopy (STM)[1]. The most appropriate and widely used of these microscopies in the study of polymer systems is atomic force microscopy (AFM), which, in many of its modes of operation, is suitable for imaging relatively soft, insulating solids, such as polymers and biological materials. In the simplest AFM modes of operation (contact and 'tapping'), topographic images representing the surface of the polymer specimen can be obtained. At the lamellar crystal level, such images have generally confirmed morphological and crystalline structures deduced from transmission electron microscopy (TEM) or X-ray studies. However, the resolution of the AFM can go beyond that easily achievable with TEM imaging of polymers. At higher resolution, AFM has in some cases revealed unpredicted surface structures. Another important characteristic of AFM for polymer studies is the ability to follow processes *in situ*. This is not usually possible in TEM owing to the sensitivity of polymers to electron-beam damage, and the usual requirement to stain or coat the polymer in order to improve the image contrast. AFM can also provide other information on certain mechanical properties of the polymer simultaneously with the topographic image information. Some of the properties accessible to the technique are local stiffness, adhesion, and friction.

 CCC 1022-1360/00/$ 17.50+.50/0

These advantages for AFM have been known for several years, and, indeed, they have been realised in several polymer systems. However, developments over the last two years are providing new and in some cases unique information on polymer structure and processes, some of which are challenging long-held theories in polymer science. We have moved into a new generation of the application of AFM to polymers.

This paper provides a brief overview of some of the work in our laboratory that we hope will highlight the capabilities of AFM in these areas, and indicate the directions that will be taken in the future. Most of the work described here concentrates on synthetic polymers, although examples are also taken from studies of biological macromolecules where work in this area is more advanced and highlights the possibilities of the technique.

High resolution imaging

For highly crystalline specimens, molecular and better resolution has been frequently observed[2-5]. Fig. 1a shows an image of the surface of a polybutene-1 film that has been prepared using the melt-spinning method of Petermann-Gohil[6]. Polybutene-1 is known to exhibit a number of different polymorphs dependent on the crystallization conditions, the stable form at room temperature being the hexagonal.

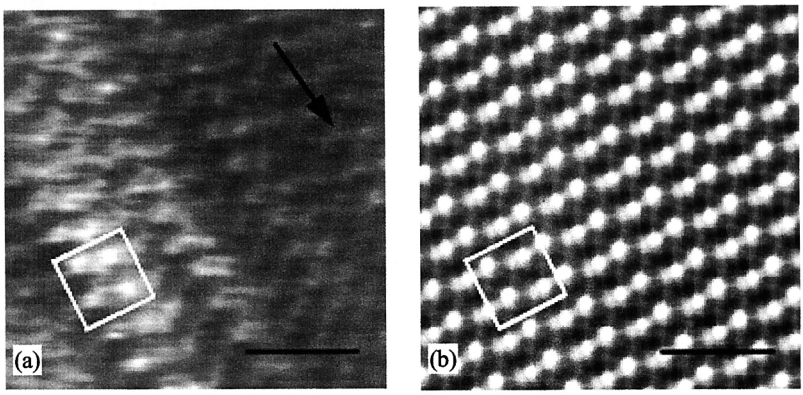

Fig. 1. a) shows an AFM contact mode topographic image of the surface of a drawn film of polybutene-1. The arrow indicates the draw direction and the box indicates an area in which the lattice is clearly visible. 1b) shows the simulated Connolly surface of the hexagonal phase of polybutene-1, showing good agreement with the AFM image.

In order to determine the polymorph present in the case imaged here, a computer model of the different crystal forms was used to produce a Connolly surface, as detailed in ref. 7. The Connolly surface corresponding to the (110) plane of the hexagonal form is shown in fig. 1b. This technique facilitates the comparison of the AFM micrograph with the surface topography expected from the crystal structure obtained using other techniques. In the case presented here it was possible to unambiguously identify the crystal as being in the hexagonal form.

In most instances, high-resolution imaging has confirmed the molecular packing on low-index planes at the surface expected from X-ray diffraction studies. However, in some cases, subtle differences in structure at the surface have been observed by AFM compared to the 3-D crystalline structure[8,9]. These differences consist of repositioning of side groups that have a different low-energy conformation when, at the surface, they do not need to satisfy the hydrogen bonding requirements of the crystalline interior. This is a form of surface relaxation or reconstruction. An example of such a surface relaxation is shown in fig. 2 for the CH_2OH group (O6) on alternate glucose-ring residues in a cellulose crystal. By comparison with simulated crystal surfaces it is possible to unambiguously identify the exposed face of the crystal as the triclinic (100) surface. However, closer examination of the AFM image reveals a subtle difference in the position of the O6 hydroxymethyl group compared to that found in the bulk. In fig. 2c the Connolly surface shows the hydroxymethyl group in the *trans-gauche* position expected in the bulk owing to H-bonding requirements. Fig. 2d shows another Connolly surface where the hydroxymethyl group has been rotated from the *trans-gauche* conformation into a *gauche-trans* conformation, clearly providing better agreement with the AFM image. This remarkable change in the position of the exocyclic hydroxyls is presumably due to changes in the hydrogen bonding when the surface is solvated. Here, we have demonstrated near-atomic resolution on this important biological specimen.

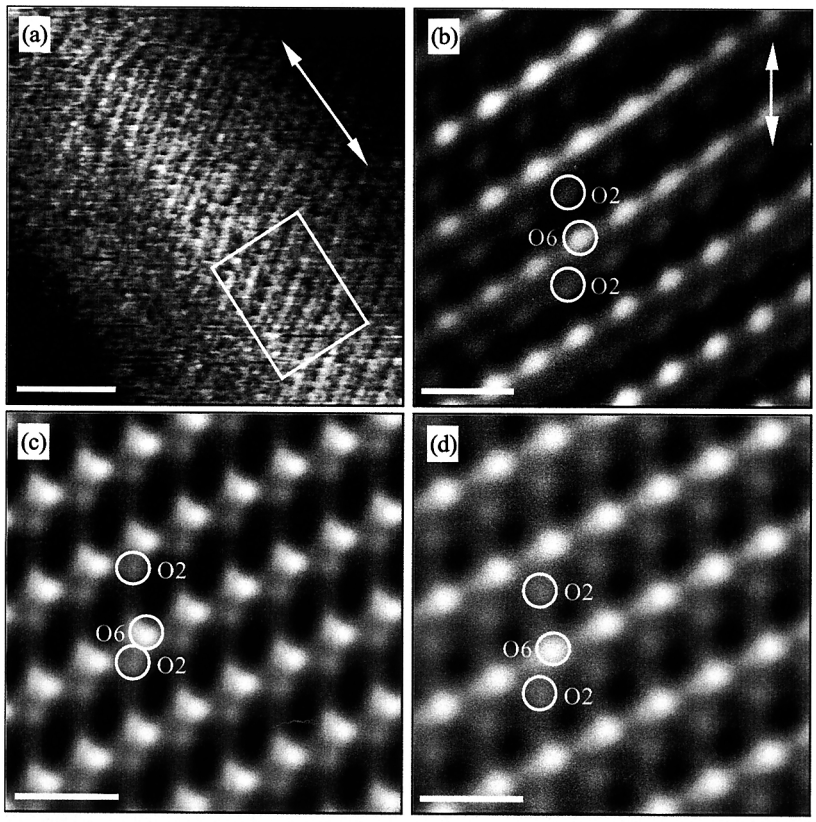

Fig. 2. a) shows an AFM topographic image of the surface of a cellulose microcrystal harvested from *Valonia ventricosa*. The scale bar represents 5nm. In fig. 2b the boxed area within fig. 1a has been rotated and Fourier filtered to remove the high frequency noise and distracting low frequency changes in topography. The scale bar represents 1nm. Figures 2c and d show simulated AFM images using the Connolly surface method as above.

Imaging in liquids – quality factor enhancement

One of the principle advantages of AFM over electron microscopy is its ability to image under liquids. In the case of biological specimens this allows the imaging of biological processes in a near physiological environment. In synthetic polymers, the following of processes such as chemical reactions, polymerisation, gelation, etching[10] etc. becomes possible. However, in many cases, the high lateral forces in contact mode damage delicate samples, necessitating the use of tapping mode. Unfortunately, in liquids, the quality factor (Q) of the cantilever is

significantly reduced by the strong hydrodynamic force between the cantilever and the fluid. In liquids a quality factor of near unity is typical, compared to ~100 in air. This reduction in Q increases the force required to drive the cantilever at a given amplitude, as the drive force is inversely proportional to the quality factor, resulting in a reduction in force sensitivity. This reduction in force sensitivity reduces the resolution that can be obtained on soft samples, and makes it impossible to image very soft materials.

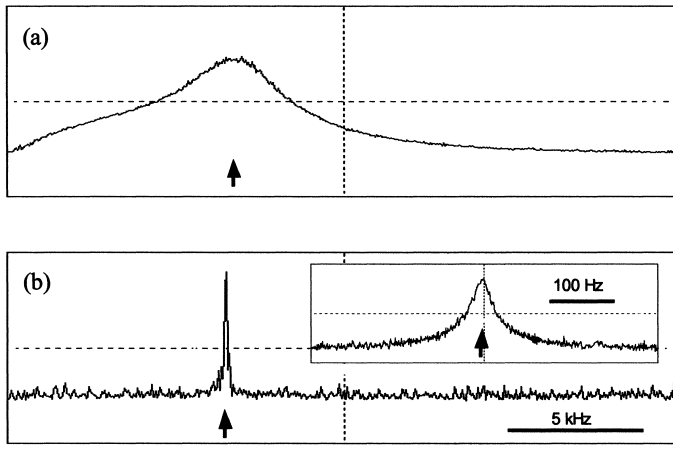

Fig. 3. A pair of frequency sweeps taken using a magnetically driven cantilever (so only the resonance of the cantilever is visible, rather than resonances within the rest of the fluid cell) in liquid. 3a) shows a standard frequency sweep. 3b) shows a frequency sweep with the Q-control on. The insert in (b) shows an enlargement of the enhanced resonant peak. The arrow marks 16.05kHz.

It has recently been found[11-13] that it is possible to enhance the effective Q of the cantilever, of particular significance when applied in liquids[14-15]. A method of Q-control has been developed in which the amplified and 90 degrees phase shifted photodiode signal is fed back into the drive signal. This adds a velocity dependent (i.e. a viscous or damping) component into the drive signal, hence reducing the effective damping factor of the cantilever progressively as resonance is approached. Fig. 3 shows examples of frequency sweeps taken with and without Q-control. The enhanced Q behaves in exactly the same way as a normal Q, and the force sensitivity of the microscope is considerably improved. This technique has already been applied to the imaging of an agarose gel[14], and to force spectroscopy[15].

We have applied this new technology to the imaging of a 30% isotactic polystyrene (iPS) decahydronapthalene (dekalin) gel under dekalin. The iPS-dekalin system has been extensively studied as it displays rich phase behaviour with at least four different gel states[16]. In order to gain sub-micron structural information in real space, it has previously been necessary to dry the gel down, with the possibility of crossing a phase line or otherwise disrupting the structure. Using enhanced Q liquid tapping we have been able to image the gel in dekalin-saturated conditions, under dekalin, obtaining images of the fully swollen gel surface. Fig. 4 shows a pair of topography images of the clear gel, or Gel II, surface, formed by quenching the solution from 140°C to 0°C and then heating to room temperature. Fig. 4a is the best image that could be obtained using standard imaging methods with this very soft system. Some fine structure is apparent, although the image is exceptionally streaky, possibly because the soft sample surface was oscillating during imaging. Fig. 4b shows an image of the same area taken with the Q-control on, with an effective Q ~ 70. The improvement in image quality is striking. Not only is the microscope now able to track the surface without the streakiness seen before, but also, the resolution of the image has been significantly enhanced. A fine, network structure, possibly of the individual crystallites, is visible.

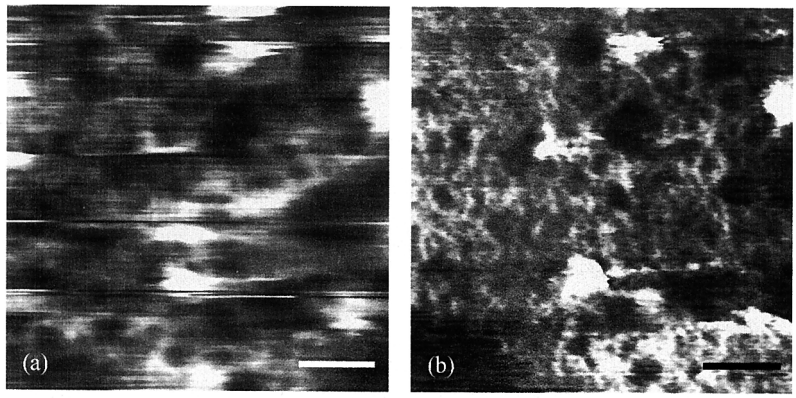

Fig. 4. A pair of images of the surface of an isotactic polystyrene gel. 4a) taken under standard imaging conditions. 4b) taken using Q-control with an effective Q of ~70. The scale bar represents 1μm.

The possibility now exists of actually imaging a gel such as the one shown above during a transition between different gel forms, as the temperature is increased. Without the force sensitivity available with active Q-control, the imaging of processes in such soft materials, under liquids, is almost impossible.

Processes

One of the principal advantages of being able to image without any complex sample preparation, such as staining or coating, is that processes can be followed in situ, in real time. This offers the unique opportunity to obtain real space information on how processes occur, and on their kinetics, with nanometre spatial resolution. In the field of synthetic polymers, this has already been extensively utilised for the study of polymer crystallization[17-22], and, to a lesser extent, crystal thickening[23] and melting[19]. The possibilities of the technique are further expanded when combined with apparatus for controlling the environment of the polymer, for example with heating stages and mechanical deformation rigs[24]. The potential for expansion in these areas is great, and in our opinion the following of processes will play an increasingly significant role in SPM research in coming years. In this section we give a brief overview of some current and recent work in our laboratory that shows some of this potential. In all of the images shown the imaging conditions were adjusted so as to just remain in repulsive mode whilst maintaining the fast scan rates necessary to follow the process of interest.

Polymer crystallization is a mature area of polymer science to which AFM can make a significant, and possibly decisive, contribution. Early studies in our laboratory of the crystallization of poly(hydroxybutyrate-co-valerate) (PHB/V) from the melt at room temperature, found an unexpected discontinuity in the growth rate when growth was observed on a lamellar scale[17]. Fig. 5 is a series of micrographs showing the growth front of a PHB/V spherulite on a lamellar scale. In this work phase imaging was used to clearly distinguish between the hard, non-adhesive crystals, and the soft, adhesive, amorphous material[25-29]. In the images shown here the lamellae can be seen both edge and flat on. Curves in the lamellae are due to the lamellar twisting that occurs in these spherulites, giving them the characteristic banded optical morphology[30]. Unfortunately, it has not as yet been possible to observe precisely how this twisting occurs. There is some indication that rather than there being a simple array of helicoids, some of the lamellae twist additionally, as if they are wrapping around a central cylinder at the same time as twisting individually. More importantly, perhaps, is the continued observation that the growth rate of the individual lamellae is not the same as that of the spherulite as a whole, but rather varies with time. Current work in our laboratory implies that this phenomenon may be more general, applying to other polymers including polyethylene, with profound implications for our understanding of polymer crystallization.

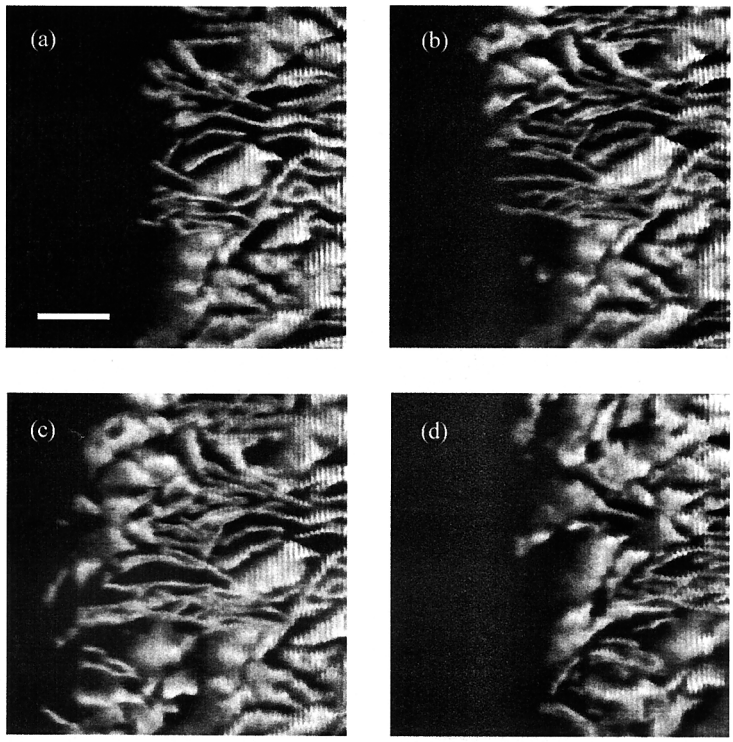

Fig. 5. A series of tapping mode phase images of the crystallization of a PHB/V spherulite taking during continuous scanning, the scan area being moved to follow the growth front. Scans started after a) 0s, b) 36s, c) 72s, d) 118s. The vertical lines down the right of the images are oscillations caused by the fast scan speeds used. The scale bar represents 100nm.

Initial AFM studies of crystallization concentrated on polymers that could be observed at[17,22], or close to[18-21], room temperature. However, most commercial polymers have melting temperatures significantly above room temperature, and are usually processed and crystallized at similar elevated temperatures. Recent work, in our laboratory and elsewhere, has started to address the crystallization of these materials, utilising microscope hot-stages[31], and high stability tip-scanned AFMs. Fig. 6 shows a series of micrographs taken during the isothermal crystallization of a thin film of polyethylene (Rigidex 50, M_w 65000, M_n 12000). In this series of images the formation of a screw dislocation is shown as the lamellae "in-fill" behind the main growth front. In fig. 6a a small nick can be seen in the leading edge of the flat-on lamella in the centre of the image. In subsequent images the branching of a daughter lamella can be seen underneath the original lamella. From examination of fig. 6d alone – after

completion of the branching process – it might have been assumed that the lower part of the lamella grew first and the spiral growth grew out afterwards. By following the process it is apparent that the chain of events was in fact the opposite of that which post-mortem examination suggests.

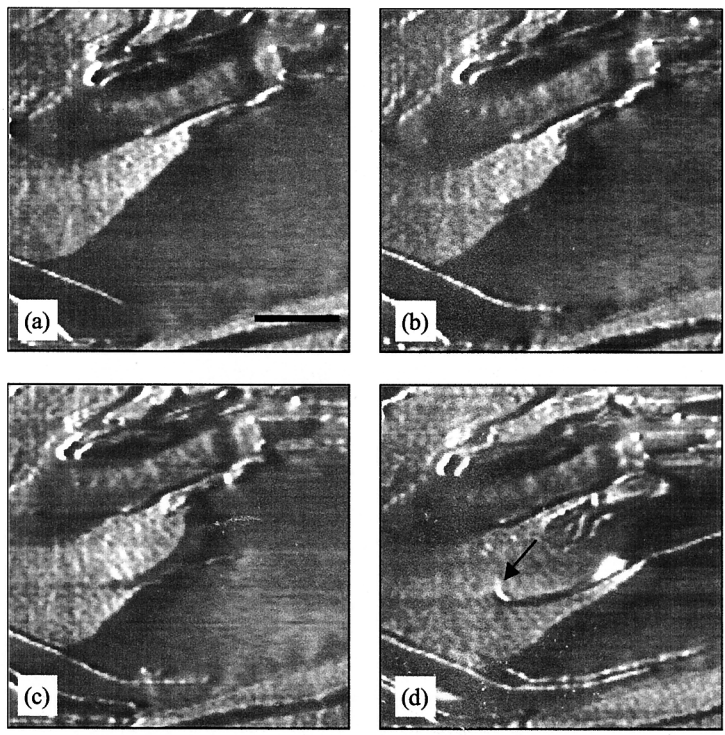

Fig. 6. A series of AFM phase images taken during the crystallization of polyethylene. Images were captured during continuous scanning. For images shown, scans started at a) 0s, b) 42s, c)126s, d) 462s. The arrow indicates the screw dislocation. The scale bar represents 500nm.

Although the study of quiescent crystallization is of considerable importance for our understanding of the fundamentals of polymer crystallization, it is not a true reflection of what occurs when polymers are processed industrially. In these situations, the polymer melts undergo severe shear and elongational flow prior to, and even during, crystallization. To gain an improved insight into these processes, we have looked at the crystallization of sheared melts[32]. Fig. 7 shows a series of images taken during the crystallization of a pair of polyethylene shish kebab crystal aggregates. The largely extended chain backbone can be clearly seen, as well as the formation and growth of the folded chain lamellar overgrowths. By

studying successive images it is apparent that, as two lamellae growing from neighbouring backbones approach each other, in some cases they appear "aware" of the presence of another crystal in front of them, and readjust their direction of growth so as to avoid a direct collision. In other instances they fuse completely, forming what appears to be a single, continuous crystal. By following the process, significant new insights into the formation of these industrially important morphologies can be gained.

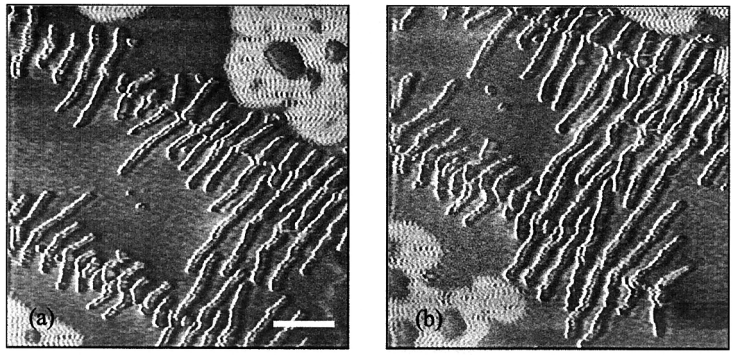

Fig. 7. A pair of AFM phase images showing the crystallization of a "shish-kebab" structure during slow cooling. 7a) taken at 132°C, b) at 131°C. The light areas in the top right and bottom left of the images are the glass substrate. Scale bar represents 300nm.

One of the unsolved puzzles of polymer behaviour is the thickening of the lamellar crystals of many polymers as they are heated towards their melting temperature. In a recent study[23] we followed this thickening process for a model system, the ultra-long alkane $C_{162}H_{326}$. In this work we found that the thickening morphology of the dried-down solution-grown crystals was dendritic, and, by following the process, we were able to attribute this structure to a barrier to thickening based on the diffusion of strain away from the thickening front. The precise uniformity of molecular weight constrains the crystals to form thicknesses that are an integer fraction of the extended chain length. However, in high polymers, no such constraints exist.

Fig. 8 shows a series of AFM height images taken during the gradual thickening during heating of a single, lozenge shaped crystal of polyethylene (Rigidex 50). It is clear from fig. 8a, taken after thickening had already begun, that thickening starts at the edges of the crystal, where there are fewer constraints to chain re-arrangement. Thickening then proceeds towards the centre of the crystal, holes opening up at the thickening front in many cases, in a similar manner to that observed during the thickening of $C_{162}H_{326}$. Finally, the crystal starts to melt.

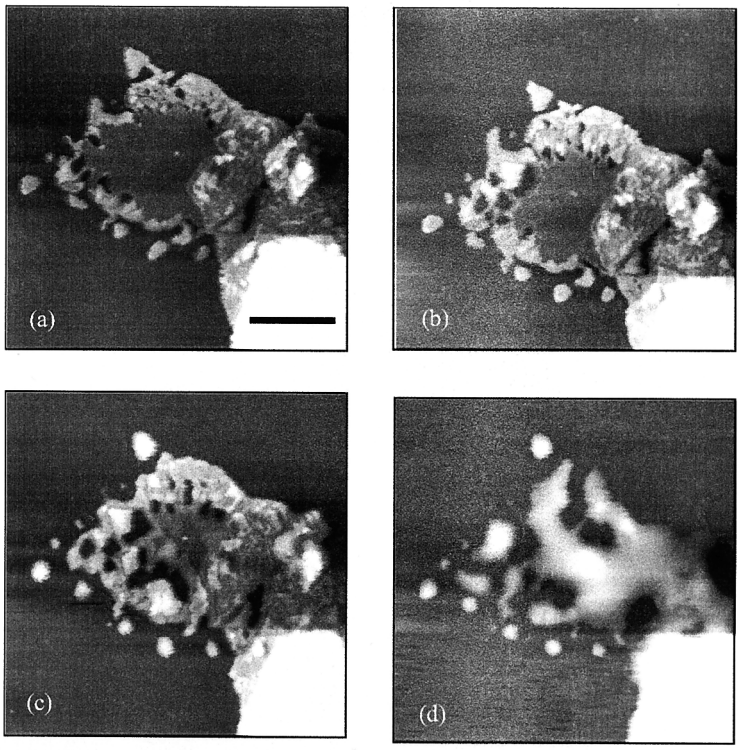

Fig. 8. A series of AFM height images taken during the slow heating of polyethylene single crystal lying on a mica substrate. 8a) ~124°C, b) ~125°C, c) ~128°C, d) ~132°C. The scale bar represents 1μm.

Surprisingly, although the thinner middle melts before much of the thickened material, some of the thickened but isolated regions around the edge of the crystal also melt early. By examining this series of images it is apparent that thickening is, in this case, a solid-state process, which occurs at a temperature considerably lower than the melting temperature of the un-thickened material. However, it is also clear that, at least in the case of these-dried down single crystals, it is not crystal thickness alone that controls melting temperature.

Another process that can be followed using AFM is polymer deformation[24,33], in which a sample is stretched under the microscope and imaged whilst held under strain (at present it is not possible to image during increases of strain).

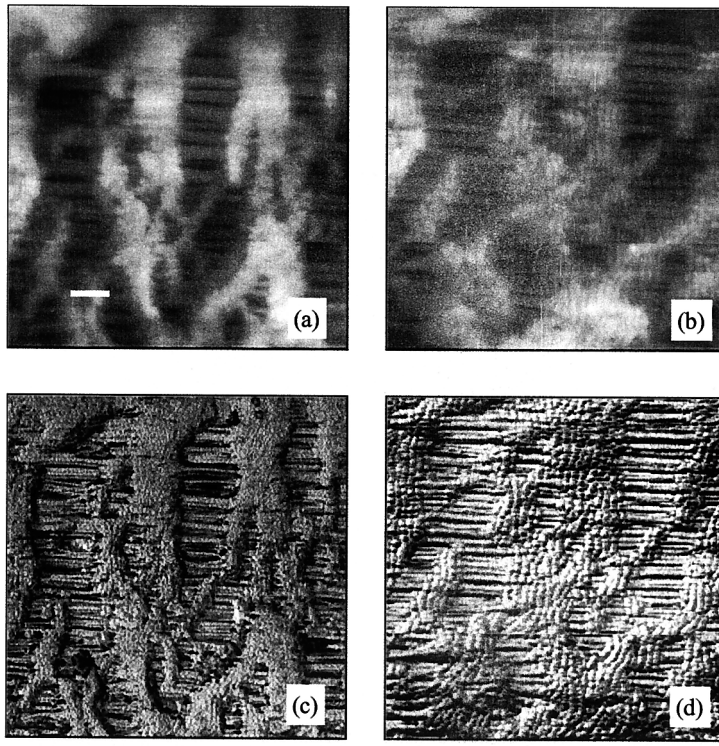

Fig. 9. A pair of topographic images with their corresponding phase images, showing the deformation of part of a hard elastic polypropylene film. 9a) and b) are height images taken before and after the application of strain. 9c) and d) are the corresponding phase images.

Fig. 9 shows two pairs of micrographs of a thin film of hard elastic polypropylene (HEPP) imaged before and after deformation. The HEPP sample has been pre-strained as part of the manufacture process and is already fibrillated before any new strain is applied. With the application of strain, it can be seen that the fibrils increase in length, do not break up into sub-fibrils, and, initially, pull little additional material from the largely un-deformed surrounding matrix. However, as further strain is applied the underlying blocky texture of the lamellae in this particular, pre-annealed material, is accentuated, due to the slight pulling apart of these blocks. It is clear that much of the elastic energy stored in the deformed material is due to the stretching of the microfibrils, before the lamellae are pulled apart.

Conclusions

In this paper we have given a brief overview of recent work in our laboratory, which, we believe, indicates the direction that SPM of crystalline polymers will take in the near future. The following of processes, such as crystallization, melting and stretching, provides the opportunity for AFM to enter a new era in which it can provide otherwise unobtainable information on a whole range of issues of both scientific and industrial importance. We have presented a few examples where new information has already been extracted from the data, which would be difficult, or impossible, to obtain by other means.

Recent advances in control of the cantilever-sample interaction when imaging in liquids, by electronic enhancement of the effective quality factor of the cantilever, open up the possibility of imaging soft materials in a liquid environment with unprecedented resolution. This provides the opportunity of accessing the fundamental length scales of many polymer systems and processes, under liquid, considerably increasing the number of possible applications of atomic force microscopy to crystalline polymers.

References

1. G. Binnig, H. Rohrer, Ch. Gerber, E. Weibel, *Appl. Phys. Letts.* **40**,178, (1982)
2. S.N. Magonov, K. Qvarnstrom, V. Elings, H.J. Cantow, *Polym. Bull.* **25**, 689, (1990)
3. H. Hansma F. Motamedi, P. Smith, P. Hansma, J.C. Wittman, *Polymer* **33**, 647, (1992)
4. D. Snetvy, J.E. Guillet, G.J. Vancso, *Polymer* **34(2)**, 429, (1993)
5. H. Schonherr, J. Vancso, *J. Pol. Sci: Part B: Pol. Phys.* **36**, 2483 (1998)
6. J. Petermann, R.M. Gohil, *J. Mater. Sci.* **14**, 2260 (1979)
7. A.K. Winkel, M.J. Miles, *Polymer Comm.* **41**, 2313 (2000)
8. A.A. Baker, W. Helbert, J. Sugiyama, M.J. Miles, *Appl. Phys. A* **66**, S559 (1998)
9. A.A. Baker, W. Helbert, J. Sugiyama, M.J. Miles, *Biophysical Journal*, **79**, 1139 (2000)
10. H. Schonherr, J. Vancso, *J. Pol. Sci: Part B: Pol. Phys.* **36** 2483 (1998)
11. U. Dürig, H.R. Steinauer, N. Blanc, *J. Appl. Phys.* **82**, 3641 (1997)
12. B. Anczykowski, J.P. Cleveland, D. Krüger, V. Elings, H. Fuchs, *Appl. Phys. A*, **66**, S885 (1998)
13. T. Sulchek, R. Hsieh, J.D. Adams, G.G. Yaralioglu, S.C. Minne, C.F. Quate, J.P. Cleveland, A. Atalar, D.M. Adderton, *Appl. Phys. Lett.* **76**, 1473 (2000)
14. J. Tamayo, A.D.L. Humphris, M.J. Miles, *Applied Physics Letters*, **77**(4), 582 (2000)
15. A.D.L. Humphris, J. Tamayo, M.J. Miles, *Langmuir*, **16**, 7891 (2000)
16. A. Keller, *Farday Discuss.* **101**, 1, (1995)
17. J.K. Hobbs, T.J. McMaster, M.J. Miles, P.J. Barham, *Polymer*, **39**(12), 2437 (1998)
18. R. Pearce, G.J. Vancso, *J. Polymer Sci. B* **36,** 2643, (1998)
19. R. Pearce, G.J. Vancso, *Polymer* **39,** 1237, (1998)
20. J.M. Schultz, & M.J. Miles, *J Polymer Sci. B*, **36**, 2311, (1998)
21. G.J. Vancso, L.G.M. Beekmans, R. Pearce, D. Trifonova, J. Varga, *J. Macromol. Sci. - Phys* **B38(5&6)**, 491 (1999)

22. L. Li, C-M Chan, J-X Li, K-M Ng, K-L Yeung, L-T Weng, *Macromolecules* **32(24)**, 8240, (1999)
23. A.K. Winkel, J.K. Hobbs, M.J. Miles, *Polymer*, **41**(25), 8791 (2000)
24. R. Godehardt, S. Rudolph, W. Lebek, S. Goerlitz, R. Adhikari, E. Allert, J. Giesemann, G.H. Michler, *J. Macromol. Sci.-Phys*, **B38(5&6)**, 817, (1999)
25. J.P. Cleveland, B. Anczykowski, A.E. Schmid, V.B. Elings, *Appl. Phys. Letts.* **72(20)**, 2613 (1998)
26. J. Tamayo, R. Garcia, *Appl. Phys. Letts.* **73(20)**, 2926 (1998)
27. G. Bar, Y. Thomann, R. Brandsch, H.J. Cantow, M.H. Whangbo *Langmuir* **13**,3807 (1997)
28. P.J. James, M. Antognozzi, J. Tamayo, T.J. McMaster, J.M. Newton and M.J. Miles submitted to *Langmuir*
29. L. Delineau, R. Brandsch, G. Bar, M.-H. Whangbo, *Surface Science* **448**, L179, (2000)
30. A. Keller, *J. Pol Sci.* **39**, 151 (1959)
31. Y.K. Godovsky, S.N. Magonov, *Langmuir*, **16(7)**, 3549 (2000)
32. J.K. Hobbs, M.J. Miles, accepted for publication in *Macromolecules*
33. S. Blakely, M. Aissaoui, T.J. McMaster, submitted to *Polymer*